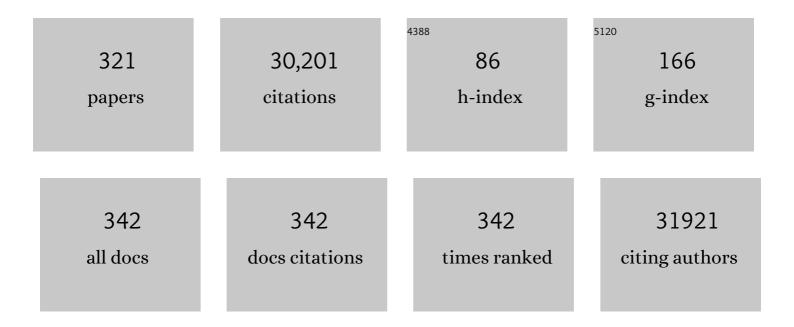
Miaofang Chi

List of Publications by Year in descending order

Source: https://exaly.com/author-pdf/7546520/publications.pdf Version: 2024-02-01



#	Article	IF	CITATIONS
1	Highly Crystalline Multimetallic Nanoframes with Three-Dimensional Electrocatalytic Surfaces. Science, 2014, 343, 1339-1343.	12.6	2,376
2	Multiple-Filled Skutterudites: High Thermoelectric Figure of Merit through Separately Optimizing Electrical and Thermal Transports. Journal of the American Chemical Society, 2011, 133, 7837-7846.	13.7	1,242
3	High electronic conductivity as the origin of lithium dendrite formation within solid electrolytes. Nature Energy, 2019, 4, 187-196.	39.5	1,099
4	Platinum-based nanocages with subnanometer-thick walls and well-defined, controllable facets. Science, 2015, 349, 412-416.	12.6	854
5	Comet 81P/Wild 2 Under a Microscope. Science, 2006, 314, 1711-1716.	12.6	848
6	Identifying surface structural changes in layered Li-excess nickel manganese oxides in high voltage lithium ion batteries: A joint experimental and theoretical study. Energy and Environmental Science, 2011, 4, 2223.	30.8	728
7	Mineralogy and Petrology of Comet 81P/Wild 2 Nucleus Samples. Science, 2006, 314, 1735-1739.	12.6	589
8	Solid Electrolyte: the Key for Highâ€Voltage Lithium Batteries. Advanced Energy Materials, 2015, 5, 1401408.	19.5	544
9	Design and Synthesis of Bimetallic Electrocatalyst with Multilayered Pt-Skin Surfaces. Journal of the American Chemical Society, 2011, 133, 14396-14403.	13.7	541
10	Palladium–platinum core-shell icosahedra with substantially enhanced activity and durability towards oxygen reduction. Nature Communications, 2015, 6, 7594.	12.8	440
11	Core/Shell Pd/FePt Nanoparticles as an Active and Durable Catalyst for the Oxygen Reduction Reaction. Journal of the American Chemical Society, 2010, 132, 7848-7849.	13.7	366
12	Efficient electrically powered CO2-to-ethanol via suppression of deoxygenation. Nature Energy, 2020, 5, 478-486.	39.5	363
13	Softâ€Templated Mesoporous Carbon arbon Nanotube Composites for High Performance Lithiumâ€ion Batteries. Advanced Materials, 2011, 23, 4661-4666.	21.0	352
14	Hard-Magnet L10-CoPt Nanoparticles Advance Fuel Cell Catalysis. Joule, 2019, 3, 124-135.	24.0	326
15	Highly Stable Silver Nanoplates for Surface Plasmon Resonance Biosensing. Angewandte Chemie - International Edition, 2012, 51, 5629-5633.	13.8	313
16	A long-life lithium-ion battery with a highly porous TiNb ₂ O ₇ anode for large-scale electrical energy storage. Energy and Environmental Science, 2014, 7, 2220-2226.	30.8	312
17	Interfacial Stability of Li Metal–Solid Electrolyte Elucidated via in Situ Electron Microscopy. Nano Letters, 2016, 16, 7030-7036.	9.1	309
18	Synthesis of Oxidation-Resistant Cupronickel Nanowires for Transparent Conducting Nanowire Networks, Nano Letters, 2012, 12, 3193-3199.	9.1	297

#	Article	IF	CITATIONS
19	Pd@Pt Core–Shell Concave Decahedra: A Class of Catalysts for the Oxygen Reduction Reaction with Enhanced Activity and Durability. Journal of the American Chemical Society, 2015, 137, 15036-15042.	13.7	296
20	Direct exfoliation of natural graphite into micrometre size few layers graphene sheets using ionic liquids. Chemical Communications, 2010, 46, 4487.	4.1	295
21	A Highly Active Titanium Dioxide Based Visibleâ€Light Photocatalyst with Nonmetal Doping and Plasmonic Metal Decoration. Angewandte Chemie - International Edition, 2011, 50, 7088-7092.	13.8	290
22	Impact Features on Stardust: Implications for Comet 81P/Wild 2 Dust. Science, 2006, 314, 1716-1719.	12.6	286
23	Understanding memristive switching via in situ characterization and device modeling. Nature Communications, 2019, 10, 3453.	12.8	275
24	Fully Alloyed Ag/Au Nanospheres: Combining the Plasmonic Property of Ag with the Stability of Au. Journal of the American Chemical Society, 2014, 136, 7474-7479.	13.7	272
25	Mn versus Al in Layered Oxide Cathodes in Lithiumâ€ion Batteries: A Comprehensive Evaluation on Longâ€Term Cyclability. Advanced Energy Materials, 2018, 8, 1703154.	19.5	260
26	Highâ€Selectivity Electrochemical Conversion of CO ₂ to Ethanol using a Copper Nanoparticle/Nâ€Doped Graphene Electrode. ChemistrySelect, 2016, 1, 6055-6061.	1.5	251
27	Correlation Between Oxygen Vacancy, Microstrain, and Cation Distribution in Lithium-Excess Layered Oxides During the First Electrochemical Cycle. Chemistry of Materials, 2013, 25, 1621-1629.	6.7	242
28	Uncovering the roles of oxygen vacancies in cation migration in lithium excess layered oxides. Physical Chemistry Chemical Physics, 2014, 16, 14665-14668.	2.8	240
29	Two-dimensional GaSe/MoSe ₂ misfit bilayer heterojunctions by van der Waals epitaxy. Science Advances, 2016, 2, e1501882.	10.3	239
30	High-entropy nanoparticles: Synthesis-structure-property relationships and data-driven discovery. Science, 2022, 376, eabn3103.	12.6	239
31	Self-organized amorphous TiO2 nanotube arrays on porous Ti foam for rechargeable lithium and sodium ion batteries. Journal of Power Sources, 2013, 222, 461-466.	7.8	235
32	A Facile Synthesis of MPd (M = Co, Cu) Nanoparticles and Their Catalysis for Formic Acid Oxidation. Nano Letters, 2012, 12, 1102-1106.	9.1	233
33	Composition-Controlled Synthesis of Bimetallic PdPt Nanoparticles and Their Electro-oxidation of Methanol. Chemistry of Materials, 2011, 23, 4199-4203.	6.7	232
34	Local electronic structure variation resulting in Li â€~filament' formation within solid electrolytes. Nature Materials, 2021, 20, 1485-1490.	27.5	226
35	Facile Synthesis of Sub-20 nm Silver Nanowires through a Bromide-Mediated Polyol Method. ACS Nano, 2016, 10, 7892-7900.	14.6	223
36	Controlled Vapor Phase Growth of Single Crystalline, Two-Dimensional GaSe Crystals with High Photoresponse. Scientific Reports, 2014, 4, 5497.	3.3	222

#	Article	IF	CITATIONS
37	Atomic-scale origin of the large grain-boundary resistance in perovskite Li-ion-conducting solid electrolytes. Energy and Environmental Science, 2014, 7, 1638.	30.8	219
38	Correlation Between Surface Chemistry and Electrocatalytic Properties of Monodisperse Pt _{<i>x</i>} Ni _{1â€<i>x</i>} Nanoparticles. Advanced Functional Materials, 2011, 21, 147-152.	14.9	218
39	Rational Design of Bi Nanoparticles for Efficient Electrochemical CO ₂ Reduction: The Elucidation of Size and Surface Condition Effects. ACS Catalysis, 2016, 6, 6255-6264.	11.2	212
40	Novel Pt/Mg(In)(Al)O catalysts for ethane and propane dehydrogenation. Journal of Catalysis, 2011, 282, 165-174.	6.2	206
41	Functional links between Pt single crystal morphology and nanoparticles with different size and shape: the oxygen reduction reaction case. Energy and Environmental Science, 2014, 7, 4061-4069.	30.8	205
42	Comparison of Comet 81P/Wild 2 Dust with Interplanetary Dust from Comets. Science, 2008, 319, 447-450.	12.6	199
43	Entropy-stabilized metal oxide solid solutions as CO oxidation catalysts with high-temperature stability. Journal of Materials Chemistry A, 2018, 6, 11129-11133.	10.3	196
44	On the Design of Highâ€Efficiency Thermoelectric Clathrates through a Systematic Crossâ€Substitution of Framework Elements. Advanced Functional Materials, 2010, 20, 755-763.	14.9	195
45	Room-Temperature Multiferroic Hexagonal <mml:math xmlns:mml="http://www.w3.org/1998/Math/MathML" display="inline"><mml:msub><mml:mi>LuFeO</mml:mi><mml:mn>3</mml:mn></mml:msub>Films. Physical Review Letters. 2013. 110. 237601.</mml:math 	7.8	195
46	Ni/Pd core/shell nanoparticles supported on graphene as a highly active and reusable catalyst for Suzuki-Miyaura cross-coupling reaction. Nano Research, 2013, 6, 10-18.	10.4	184
47	Crystal Structural Effect of AuCu Alloy Nanoparticles on Catalytic CO Oxidation. Journal of the American Chemical Society, 2017, 139, 8846-8854.	13.7	181
48	Polyol Synthesis of Ultrathin Pd Nanowires via Attachmentâ€Based Growth and Their Enhanced Activity towards Formic Acid Oxidation. Advanced Functional Materials, 2014, 24, 131-139.	14.9	173
49	Interphase Morphology between a Solid-State Electrolyte and Lithium Controls Cell Failure. ACS Energy Letters, 2019, 4, 591-599.	17.4	168
50	Synthesis and Characterization of Multimetallic Pd/Au and Pd/Au/FePt Core/Shell Nanoparticles. Angewandte Chemie - International Edition, 2010, 49, 9368-9372.	13.8	167
51	Synthesis and Catalytic Properties of Au–Pd Nanoflowers. ACS Nano, 2011, 5, 6119-6127.	14.6	163
52	Phosphonium-Organophosphate Ionic Liquids as Lubricant Additives: Effects of Cation Structure on Physicochemical and Tribological Characteristics. ACS Applied Materials & Interfaces, 2014, 6, 22585-22593.	8.0	163
53	Comparison of an oil-miscible ionic liquid and ZDDP as a lubricant anti-wear additive. Tribology International, 2014, 71, 88-97.	5.9	161
54	Surface faceting and elemental diffusion behaviour at atomic scale for alloy nanoparticles during in situ annealing. Nature Communications, 2015, 6, 8925.	12.8	159

#	Article	IF	CITATIONS
55	Denary oxide nanoparticles as highly stable catalysts for methane combustion. Nature Catalysis, 2021, 4, 62-70.	34.4	153
56	Lab-in-a-Shell: Encapsulating Metal Clusters for Size Sieving Catalysis. Journal of the American Chemical Society, 2014, 136, 11260-11263.	13.7	152
57	Long-Term Cyclability of NCM-811 at High Voltages in Lithium-Ion Batteries: an In-Depth Diagnostic Study. Chemistry of Materials, 2020, 32, 7796-7804.	6.7	152
58	Multimetallic Core/Interlayer/Shell Nanostructures as Advanced Electrocatalysts. Nano Letters, 2014, 14, 6361-6367.	9.1	146
59	Comparing Wild 2 particles to chondrites and IDPs. Meteoritics and Planetary Science, 2008, 43, 261-272.	1.6	136
60	Electrical and thermal conductivity of low temperature CVD graphene: the effect of disorder. Nanotechnology, 2011, 22, 275716.	2.6	132
61	Integrated Nano-Domains of Disordered and Ordered Spinel Phases in LiNi _{0.5} Mn _{1.5} O ₄ for Li-Ion Batteries. Chemistry of Materials, 2014, 26, 4377-4386.	6.7	132
62	Rational Development of Ternary Alloy Electrocatalysts. Journal of Physical Chemistry Letters, 2012, 3, 1668-1673.	4.6	130
63	Interfaces in Heterogeneous Catalysts: Advancing Mechanistic Understanding through Atomic-Scale Measurements. Accounts of Chemical Research, 2017, 50, 787-795.	15.6	128
64	Efficient upgrading of CO to C3 fuel using asymmetric C-C coupling active sites. Nature Communications, 2019, 10, 5186.	12.8	127
65	Synthesis of Homogeneous Pt-Bimetallic Nanoparticles as Highly Efficient Electrocatalysts. ACS Catalysis, 2011, 1, 1355-1359.	11.2	124
66	Ru Octahedral Nanocrystals with a Face-Centered Cubic Structure, {111} Facets, Thermal Stability up to 400 °C, and Enhanced Catalytic Activity. Journal of the American Chemical Society, 2019, 141, 7028-7036.	13.7	122
67	Controlling the Surface Oxidation of Cu Nanowires Improves Their Catalytic Selectivity and Stability toward C ₂₊ Products in CO ₂ Reduction. Angewandte Chemie - International Edition, 2021, 60, 1909-1915.	13.8	122
68	In-Plane Heterojunctions Enable Multiphasic Two-Dimensional (2D) MoS ₂ Nanosheets As Efficient Photocatalysts for Hydrogen Evolution from Water Reduction. ACS Catalysis, 2016, 6, 6723-6729.	11.2	116
69	Excellent Stability of a Lithiumâ€lonâ€Conducting Solid Electrolyte upon Reversible Li ⁺ /H ⁺ Exchange in Aqueous Solutions. Angewandte Chemie - International Edition, 2015, 54, 129-133.	13.8	112
70	Understanding the Low-Voltage Hysteresis of Anionic Redox in Na ₂ Mn ₃ O ₇ . Chemistry of Materials, 2019, 31, 3756-3765.	6.7	112
71	Quantitative Analysis of the Reduction Kinetics Responsible for the One-Pot Synthesis of Pd–Pt Bimetallic Nanocrystals with Different Structures. Journal of the American Chemical Society, 2016, 138, 12263-12270.	13.7	111
72	Synthesis and Characterization of Ru Cubic Nanocages with a Face-Centered Cubic Structure by Templating with Pd Nanocubes. Nano Letters, 2016, 16, 5310-5317.	9.1	110

#	Article	IF	CITATIONS
73	Probing the electrode/electrolyte interface in the lithium excess layered oxide Li1.2Ni0.2Mn0.6O2. Physical Chemistry Chemical Physics, 2013, 15, 11128.	2.8	107
74	Tertiary and Quaternary Ammonium-Phosphate Ionic Liquids as Lubricant Additives. Tribology Letters, 2016, 63, 1.	2.6	107
75	A refractory inclusion returned by Stardust from comet 81P/Wild 2. Meteoritics and Planetary Science, 2008, 43, 1861-1877.	1.6	106
76	Direct Assembly of Hydrophobic Nanoparticles to Multifunctional Structures. Nano Letters, 2011, 11, 3404-3412.	9.1	104
77	Van der Waals Epitaxial Growth of Two-Dimensional Single-Crystalline GaSe Domains on Graphene. ACS Nano, 2015, 9, 8078-8088.	14.6	103
78	Extreme mixing in nanoscale transition metal alloys. Matter, 2021, 4, 2340-2353.	10.0	102
79	Ptâ€ŀrâ€₽d Trimetallic Nanocages as a Dual Catalyst for Efficient Oxygen Reduction and Evolution Reactions in Acidic Media. Advanced Energy Materials, 2020, 10, 1904114.	19.5	100
80	Synthesis and characterization of a new catalyst Pt/Mg(Ga)(Al)O for alkane dehydrogenation. Journal of Catalysis, 2010, 274, 192-199.	6.2	97
81	High voltage stability of LiCoO2 particles with a nano-scale Lipon coating. Electrochimica Acta, 2011, 56, 6573-6580.	5.2	91
82	Supported bimetallic PdAu nanoparticles with superior electrocatalytic activity towards methanol oxidation. Journal of Materials Chemistry A, 2013, 1, 9157.	10.3	91
83	Iridiumâ€Based Cubic Nanocages with 1.1â€nmâ€Thick Walls: A Highly Efficient and Durable Electrocatalyst for Water Oxidation in an Acidic Medium. Angewandte Chemie - International Edition, 2019, 58, 7244-7248.	13.8	89
84	Synthesis–Structure–Property Relations in Layered, "Li-excess―Oxides Electrode Materials Li[Li[sub 1/3â~2x/3]Ni[sub x]Mn[sub 2/3â~x/3]]O[sub 2] (x=1/3, 1/4, and 1/5). Journal of the Electrochemical Society, 2010, 157, A1202.	2.9	88
85	A "Shipâ€Inâ€Aâ€Bottle―Approach to Synthesis of Polymer Dots@Silica or Polymer Dots@Carbon Coreâ€S Nanospheres. Advanced Materials, 2012, 24, 6017-6021.	he 21.0	88
86	Active and Stable Embedded Au@CeO ₂ Catalysts for Preferential Oxidation of CO. Chemistry of Materials, 2010, 22, 4335-4345.	6.7	87
87	Understanding the Role of NH ₄ F and Al ₂ O ₃ Surface Co-modification on Lithium-Excess Layered Oxide Li _{1.2} Ni _{0.2} Mn _{0.6} O ₂ . ACS Applied Materials & amp; Interfaces. 2015. 7, 19189-19200.	8.0	87
88	Phase Transitions, Phase Coexistence, and Piezoelectric Switching Behavior in Highly Strained BiFeO ₃ Films. Advanced Materials, 2013, 25, 5561-5567.	21.0	84
89	Sub-Ãngstrom electric field measurements on a universal detector in a scanning transmission electron microscope. Advanced Structural and Chemical Imaging, 2018, 4, 10.	4.0	84
90	Ternary CoPtAu Nanoparticles as a General Catalyst for Highly Efficient Electroâ€oxidation of Liquid Fuels. Angewandte Chemie - International Edition, 2019, 58, 11527-11533.	13.8	83

#	Article	IF	CITATIONS
91	Lithiumâ€lon Batteries: Solid Electrolyte: the Key for Highâ€Voltage Lithium Batteries (Adv. Energy Mater.) Tj ETC	Qq110.7	84314 rgBT
92	Probing the initiation of voltage decay in Li-rich layered cathode materials at the atomic scale. Journal of Materials Chemistry A, 2015, 3, 5385-5391.	10.3	81
93	Stabilizing gold clusters by heterostructured transition-metal oxide–mesoporous silica supports for enhanced catalytic activities for CO oxidation. Chemical Communications, 2012, 48, 11413.	4.1	80
94	Kinetically Controlled Synthesis of Pd–Cu Janus Nanocrystals with Enriched Surface Structures and Enhanced Catalytic Activities toward CO ₂ Reduction. Journal of the American Chemical Society, 2021, 143, 149-162.	13.7	77
95	Advanced analytical electron microscopy for lithium-ion batteries. NPG Asia Materials, 2015, 7, e193-e193.	7.9	76
96	Anisotropic Strain Tuning of L1 ₀ Ternary Nanoparticles for Oxygen Reduction. Journal of the American Chemical Society, 2020, 142, 19209-19216.	13.7	76
97	Core–Shell Nanostructured Cobalt–Platinum Electrocatalysts with Enhanced Durability. ACS Catalysis, 2018, 8, 35-42.	11.2	72
98	An ultrastable heterostructured oxide catalyst based on high-entropy materials: A new strategy toward catalyst stabilization via synergistic interfacial interaction. Applied Catalysis B: Environmental, 2020, 276, 119155.	20.2	72
99	Tailored recovery of carbons from waste tires for enhanced performance as anodes in lithium-ion batteries. RSC Advances, 2014, 4, 38213.	3.6	70
100	Enhanced Photoreversible Color Switching of Redox Dyes Catalyzed by Bariumâ€Đoped TiO ₂ Nanocrystals. Angewandte Chemie - International Edition, 2015, 54, 1321-1326.	13.8	70
101	Catalytic System Based on Sub-2 nm Pt Particles and Its Extraordinary Activity and Durability for Oxygen Reduction. Nano Letters, 2019, 19, 4997-5002.	9.1	68
102	Synthesis of Ru Icosahedral Nanocages with a Face-Centered-Cubic Structure and Evaluation of Their Catalytic Properties. ACS Catalysis, 2018, 8, 6948-6960.	11.2	66
103	Heterostructured catalysts prepared by dispersing Au@Fe2O3 core–shell structures on supports and their performance in CO oxidation. Catalysis Today, 2011, 160, 87-95.	4.4	65
104	Self-aligned Cu–Si core–shell nanowire array as a high-performance anode for Li-ion batteries. Journal of Power Sources, 2012, 198, 312-317.	7.8	65
105	A novel method combining additive manufacturing and alloy infiltration for NdFeB bonded magnet fabrication. Journal of Magnetism and Magnetic Materials, 2017, 438, 163-167.	2.3	65
106	Facile Synthesis and Characterization of Pd@Ir _{<i>n</i>L} (<i>n</i> = 1–4) Core–Shell Nanocubes for Highly Efficient Oxygen Evolution in Acidic Media. Chemistry of Materials, 2019, 31, 5867-5875.	6.7	65
107	Unrivaled combination of surface area and pore volume in micelle-templated carbon for supercapacitor energy storage. Journal of Materials Chemistry A, 2017, 5, 13511-13525.	10.3	63
108	Mesoporous carbon–Cr2O3 composite as an anode material for lithium ion batteries. Journal of Power Sources, 2012, 205, 495-499.	7.8	62

#	Article	IF	CITATIONS
109	In situ X-ray diffraction study of the lithium excess layered oxide compound Li[Li0.2Ni0.2Mn0.6]O2 during electrochemical cycling. Solid State Ionics, 2012, 207, 44-49.	2.7	62
110	Controlled Synthesis of Nanosized Palladium icosahedra and Their Catalytic Activity towards Formicâ€Acid Oxidation. ChemSusChem, 2013, 6, 1923-1930.	6.8	62
111	Big Data Analytics for Scanning Transmission Electron Microscopy Ptychography. Scientific Reports, 2016, 6, 26348.	3.3	62
112	Plating Precious Metals on Nonprecious Metal Nanoparticles for Sustainable Electrocatalysts. Nano Letters, 2017, 17, 3391-3395.	9.1	61
113	Island Growth in the Seed-Mediated Overgrowth of Monometallic Colloidal Nanostructures. CheM, 2017, 3, 678-690.	11.7	61
114	Confined Lithium–Sulfur Reactions in Narrow-Diameter Carbon Nanotubes Reveal Enhanced Electrochemical Reactivity. ACS Nano, 2018, 12, 9775-9784.	14.6	61
115	Dynamic scan control in STEM: spiral scans. Advanced Structural and Chemical Imaging, 2016, 2, .	4.0	59
116	Co:CdS Diluted Magnetic Semiconductor Nanoparticles: Radiation Synthesis, Dopantâ^'Defect Complex Formation, and Unexpected Magnetism. Chemistry of Materials, 2008, 20, 440-446.	6.7	56
117	Facile Synthesis of Ru-Based Octahedral Nanocages with Ultrathin Walls in a Face-Centered Cubic Structure. Chemistry of Materials, 2017, 29, 9227-9237.	6.7	55
118	Construction of a Nanoporous Highly Crystalline Hexagonal Boron Nitride from an Amorphous Precursor for Catalytic Dehydrogenation. Angewandte Chemie - International Edition, 2019, 58, 10626-10630.	13.8	55
119	Epitaxial Nanosheet–Nanowire Heterostructures. Nano Letters, 2013, 13, 948-953.	9.1	54
120	Role of LiCoO ₂ Surface Terminations in Oxygen Reduction and Evolution Kinetics. Journal of Physical Chemistry Letters, 2015, 6, 1357-1362.	4.6	54
121	Nanostructure and Composition of Tribo-Boundary Films Formed in Ionic Liquid Lubrication. Tribology Letters, 2011, 43, 205-211.	2.6	53
122	Understanding the Thermal Stability of Palladium–Platinum Core–Shell Nanocrystals by <i>In Situ</i> Transmission Electron Microscopy and Density Functional Theory. ACS Nano, 2017, 11, 4571-4581.	14.6	53
123	A mutation in calsequestrin, CASQ2D307H, impairs Sarcoplasmic Reticulum Ca2+ handling and causes complex ventricular arrhythmias in mice. Cardiovascular Research, 2007, 75, 69-78.	3.8	52
124	A Perspective on Coatings to Stabilize High-Voltage Cathodes: LiMn _{1.5} Ni _{0.5} O ₄ with Sub-Nanometer Lipon Cycled with LiPF ₆ Electrolyte. Journal of the Electrochemical Society, 2013, 160, A3113-A3125.	2.9	51
125	A Memristor with Low Switching Current and Voltage for 1S1R Integration and Array Operation. Advanced Electronic Materials, 2020, 6, 1901411.	5.1	51
126	Facile synthesis of Ag@Au core–sheath nanowires with greatly improved stability against oxidation. Chemical Communications, 2017, 53, 1965-1968.	4.1	50

#	Article	IF	CITATIONS
127	Understanding the Impact of Surface Reconstruction of Perovskite Catalysts on CH ₄ Activation and Combustion. ACS Catalysis, 2018, 8, 10306-10315.	11.2	50
128	<i>In Situ</i> Strong Metal–Support Interaction (SMSI) Affects Catalytic Alcohol Conversion. ACS Catalysis, 2021, 11, 1938-1945.	11.2	50
129	Site Mixing for Engineering Magnetic Topological Insulators. Physical Review X, 2021, 11, .	8.9	50
130	Effect of Surface Structure of TiO ₂ Nanoparticles on CO ₂ Adsorption and SO ₂ Resistance. ACS Sustainable Chemistry and Engineering, 2017, 5, 9295-9306.	6.7	49
131	Multi-principal elemental intermetallic nanoparticles synthesized via a disorder-to-order transition. Science Advances, 2022, 8, eabm4322.	10.3	49
132	Elucidating the mobility of H ⁺ and Li ⁺ ions in (Li _{6.25â^'x} H _x Al _{0.25})La ₃ Zr ₂ O ₁₂ <i> neutron and electron spectroscopy. Energy and Environmental Science, 2019, 12, 945-951.</i>	×V\$NETX\$I>CC	rr el ative
133	Growth and structure of PbVO3 thin films. Applied Physics Letters, 2007, 90, 062903.	3.3	47
134	Fabrication of Subâ€Micrometerâ€Thick Solid Electrolyte Membranes of βâ€Li ₃ PS ₄ via Tiled Assembly of Nanoscale, Plateâ€Like Building Blocks. Advanced Energy Materials, 2018, 8, 1800014.	19.5	47
135	Ruthenium Nanoframes in the Face-Centered Cubic Phase: Facile Synthesis and Their Enhanced Catalytic Performance. ACS Nano, 2019, 13, 7241-7251.	14.6	47
136	Mesoscopic Framework Enables Facile Ionic Transport in Solid Electrolytes for Li Batteries. Advanced Energy Materials, 2016, 6, 1600053.	19.5	46
137	Pdâ€Ru Alloy Nanocages with a Face entered Cubic Structure and Their Enhanced Activity toward the Oxidation of Ethylene Glycol and Glycerol. Small Methods, 2020, 4, 1900843.	8.6	46
138	Revealing the Preferred Interlayer Orientations and Stackings of Twoâ€Dimensional Bilayer Gallium Selenide Crystals. Angewandte Chemie - International Edition, 2015, 54, 2712-2717.	13.8	45
139	In situ TEM observation of the electrochemical lithiation of N-doped anatase TiO ₂ nanotubes as anodes for lithium-ion batteries. Journal of Materials Chemistry A, 2017, 5, 20651-20657.	10.3	45
140	Charge Separation in a Niobate Nanosheet Photocatalyst Studied with Photochemical Labeling. Langmuir, 2010, 26, 7254-7261.	3.5	44
141	Graphitized hollow carbon spheres and yolk-structured carbon spheres fabricated by metal-catalyst-free chemical vapor deposition. Carbon, 2016, 101, 57-61.	10.3	44
142	Maximizing the Catalytic Performance of Pd@Au _x Pd _{1â^'<i>x</i>} Nanocubes in H ₂ O ₂ Production by Reducing Shell Thickness to Increase Compositional Stability. Angewandte Chemie - International Edition, 2021, 60, 19643-19647.	13.8	44
143	Rational Defect Introduction in Silicon Nanowires. Nano Letters, 2013, 13, 1928-1933.	9.1	43
144	Reciprocal Salt Flux Growth of LiFePO ₄ Single Crystals with Controlled Defect Concentrations. Chemistry of Materials, 2013, 25, 4574-4584.	6.7	43

#	Article	lF	CITATIONS
145	Comparison of the tribological behavior of steel–steel and Si3N4–steel contacts in lubricants with ZDDP or ionic liquid. Wear, 2014, 319, 172-183.	3.1	43
146	Direct in Situ Observation and Analysis of the Formation of Palladium Nanocrystals with High-Index Facets. Nano Letters, 2018, 18, 7004-7013.	9.1	42
147	Solution-Phase Synthesis of PdH _{0.706} Nanocubes with Enhanced Stability and Activity toward Formic Acid Oxidation. Journal of the American Chemical Society, 2022, 144, 2556-2568.	13.7	42
148	Improving corrosion resistance of AZ31B magnesium alloy via a conversion coating produced by a protic ammonium-phosphate ionic liquid. Thin Solid Films, 2014, 568, 44-51.	1.8	41
149	New Chemical Route for the Synthesis of β-Na _{0.33} V ₂ O ₅ and Its Fully Reversible Li Intercalation. ACS Applied Materials & Interfaces, 2015, 7, 7025-7032.	8.0	41
150	Antisite Pairs Suppress the Thermal Conductivity of BAs. Physical Review Letters, 2018, 121, 105901.	7.8	41
151	Facile One-Pot Synthesis of Pd@Pt _{1L} Octahedra with Enhanced Activity and Durability toward Oxygen Reduction. Chemistry of Materials, 2019, 31, 1370-1380.	6.7	41
152	Unveiling the Role of Al ₂ O ₃ in Preventing Surface Reconstruction During High-Voltage Cycling of Lithium-Ion Batteries. ACS Applied Energy Materials, 2019, 2, 1308-1313.	5.1	41
153	Practical application of fractional Brownian Motion and noise to synthetic hydrology. Water Resources Research, 1973, 9, 1523-1533.	4.2	39
154	TiO2 nanotube arrays grown in ionic liquids: high-efficiency in photocatalysis and pore-widening. Journal of Materials Chemistry, 2011, 21, 9487.	6.7	38
155	Pt3Re alloy nanoparticles as electrocatalysts for the oxygen reduction reaction. Nano Energy, 2016, 20, 202-211.	16.0	38
156	Tire-derived carbon for catalytic preparation of biofuels from feedstocks containing free fatty acids. Carbon Resources Conversion, 2018, 1, 165-173.	5.9	38
157	Infrared transitions in strainedâ€layer GexSi1â^'x/Si. Journal of Applied Physics, 1994, 75, 8012-8021.	2.5	37
158	Elucidating Interfacial Stability between Lithium Metal Anode and Li Phosphorus Oxynitride via <i>In Situ</i> Electron Microscopy. Nano Letters, 2021, 21, 151-157.	9.1	36
159	Abnormally Low Activation Energy in Cubic Na ₃ SbS ₄ Superionic Conductors. Chemistry of Materials, 2020, 32, 2264-2271.	6.7	35
160	Structural variability of edge dislocations in a SrTiO ₃ low-angle [001] tilt grain boundary. Journal of Materials Research, 2009, 24, 2191-2199.	2.6	34
161	Probing Electrochemical Cycling Stability of Li-ion Cathode Materials at Atomic-scale. Microscopy and Microanalysis, 2014, 20, 452-453.	0.4	33
162	Enhanced Thermoelectric Performance in Cu-Intercalated BiTeI by Compensation Weakening Induced Mobility Improvement. Scientific Reports, 2015, 5, 14319.	3.3	33

#	Article	IF	CITATIONS
163	Nonequilibrium Synthesis of TiO ₂ Nanoparticle "Building Blocks―for Crystal Growth by Sequential Attachment in Pulsed Laser Deposition. Nano Letters, 2017, 17, 4624-4633.	9.1	33
164	The origin of refractory minerals in comet 81P/Wild 2. Geochimica Et Cosmochimica Acta, 2009, 73, 7150-7161.	3.9	32
165	Evidence for and mitigation of the encapsulation of gold nanoparticles within silica supports upon high-temperature treatment of Au/SiO2 catalysts: Implication to catalyst deactivation. Applied Catalysis A: General, 2010, 386, 147-156.	4.3	32
166	Feature extraction via similarity search: application to atom finding and denoising in electron and scanning probe microscopy imaging. Advanced Structural and Chemical Imaging, 2018, 4, 3.	4.0	31
167	A new trick for an old support: Stabilizing gold single atoms on LaFeO3 perovskite. Applied Catalysis B: Environmental, 2020, 261, 118178.	20.2	31
168	Atomic Resolution of the Structure of a Metal–Support Interface: Triosmium Clusters on MgO(110). Angewandte Chemie - International Edition, 2010, 49, 10089-10092.	13.8	30
169	From Core–Shell to Alloys: The Preparation and Characterization of Solution-Synthesized AuPd Nanoparticle Catalysts. Journal of Physical Chemistry C, 2013, 117, 17557-17566.	3.1	30
170	Activation of Dodecanethiol-Capped Gold Catalysts for CO Oxidation by Treatment with KMnO4 or K2MnO4. Catalysis Letters, 2010, 136, 209-221.	2.6	29
171	Self-Assembled Framework Formed During Lithiation of SnS ₂ Nanoplates Revealed by in Situ Electron Microscopy. Accounts of Chemical Research, 2017, 50, 1513-1520.	15.6	29
172	Photothermal transformation of Au–Ag nanocages under pulsed laser irradiation. Nanoscale, 2019, 11, 3013-3020.	5.6	29
173	Swellingâ€Induced Symmetry Breaking: A Versatile Approach to the Scalable Production of Colloidal Particles with a Janus Structure. Angewandte Chemie - International Edition, 2021, 60, 12980-12984.	13.8	28
174	A Theory-Guided X-ray Absorption Spectroscopy Approach for Identifying Active Sites in Atomically Dispersed Transition-Metal Catalysts. Journal of the American Chemical Society, 2021, 143, 20144-20156.	13.7	28
175	Interplay between Defect Propagation and Surface Hydrogen in Silicon Nanowire Kinking Superstructures. ACS Nano, 2014, 8, 3829-3835.	14.6	27
176	Facile Synthesis of Rhodium Icosahedra with Controlled Sizes up to 12â€nm. ChemNanoMat, 2016, 2, 61-66.	2.8	26
177	Kinetically Controlled Synthesis of Rhodium Nanocrystals with Different Shapes and a Comparison Study of Their Thermal and Catalytic Properties. Journal of the American Chemical Society, 2021, 143, 6293-6302.	13.7	26
178	Approximate Method of Determining the Cutoff Frequencies of Waveguides of Arbitrary Cross Section (Correspondence). IEEE Transactions on Microwave Theory and Techniques, 1964, 12, 248-249.	4.6	25
179	Growth diagram and magnetic properties of hexagonal LuFe <mmi:math xmlns:mml="http://www.w3.org/1998/Math/MathML" display="inline"><mml:msub><mml:mrow /><mml:mn>2</mml:mn></mml:mrow </mml:msub>O<mml:math xmlns:mml="http://www.w3.org/1998/Math/MathML" display="inline"><mml:msub><mml:mrow< td=""><td>3.2</td><td>25</td></mml:mrow<></mml:msub></mml:math </mmi:math 	3.2	25
180	Ferroelectric Selfâ€Poling, Switching, and Monoclinic Domain Configuration in BiFeO ₃ Thin Films. Advanced Functional Materials, 2016, 26, 5166-5173.	14.9	25

#	Article	IF	CITATIONS
181	New promising lithium malonatoborate salts for high voltage lithium ion batteries. Journal of Materials Chemistry A, 2017, 5, 1233-1241.	10.3	25
182	Defect Engineering of Ceria Nanocrystals for Enhanced Catalysis via a High-Entropy Oxide Strategy. ACS Central Science, 2022, 8, 1081-1090.	11.3	25
183	Response of oddly-stiffened circular cylindrical shells. Journal of Sound and Vibration, 1971, 17, 187-206.	3.9	24
184	Mesoporous delafossite CuCrO ₂ and spinel CuCr ₂ O ₄ : synthesis and catalysis. Nanotechnology, 2013, 24, 345704.	2.6	24
185	Direct visualization of anionic electrons in an electride reveals inhomogeneities. Science Advances, 2021, 7, .	10.3	24
186	Silica encapsulated heterostructure catalyst of Pt nanoclusters on hematite nanocubes: synthesis and reactivity. Journal of Materials Chemistry, 2010, 20, 2013.	6.7	23
187	Atomic scale analysis of the effect of the SiO2 passivation treatment on InAs/GaSb superlattice mesa sidewall. Applied Physics Letters, 2008, 93, .	3.3	21
188	Atomically Resolved Site-Isolated Catalyst on MgO: Mononuclear Osmium Dicarbonyls formed from Os ₃ (CO) ₁₂ . Journal of Physical Chemistry Letters, 2012, 3, 1865-1871.	4.6	21
189	Fundamental Relationship of Microstructure and Ionic Conductivity of Amorphous LLTO as Solid Electrolyte Material. Journal of the Electrochemical Society, 2019, 166, A515-A520.	2.9	21
190	Evidence of Bilevel Solubility in the Bimodal Microstructure of TiO2-Doped Alumina. Journal of the American Ceramic Society, 2003, 86, 1953-1955.	3.8	20
191	Revealing the Structural Stability and Na-Ion Mobility of 3D Superionic Conductor Na ₃ SbS ₄ at Extremely Low Temperatures. ACS Applied Energy Materials, 2018, 1, 7028-7034.	5.1	20
192	Migration of Iron Oxide Nanoparticle through a Silica Shell by the Redox-Buffering Effect. ACS Nano, 2018, 12, 10949-10956.	14.6	20
193	Charge Transport Modulation in PbSe Nanocrystal Solids by Au _{<i>x</i>} Ag _{1–<i>x</i>} Nanoparticle Doping. ACS Nano, 2018, 12, 9091-9100.	14.6	20
194	Multiple Promotional Effects of Vanadium Oxide on Boron Nitride for Oxidative Dehydrogenation of Propane. Jacs Au, 2022, 2, 1096-1104.	7.9	20
195	Understanding the Stability of Ptâ€Based Nanocages under Thermal Stress Using <i>In Situ</i> Electron Microscopy. ChemNanoMat, 2018, 4, 112-117.	2.8	19
196	Emerging Electron Microscopy Techniques for Probing Functional Interfaces in Energy Materials. Angewandte Chemie - International Edition, 2020, 59, 1384-1396.	13.8	19
197	The interplay between surface facet and reconstruction on isopropanol conversion over SrTiO3 nanocrystals. Journal of Catalysis, 2020, 384, 49-60.	6.2	19
198	Measuring and directing charge transfer in heterogenous catalysts. Nature Communications, 2022, 13, .	12.8	19

#	Article	IF	CITATIONS
199	In situ growth synthesis of heterostructured LnPO4–SiO2 (Ln = La, Ce, and Eu) mesoporous materials as supports for small gold particles used in catalytic CO oxidation. Journal of Materials Chemistry, 2012, 22, 25227.	6.7	18
200	Scalable Synthesis of Palladium Icosahedra in Plug Reactors for the Production of Oxygen Reduction Reaction Catalysts. ChemCatChem, 2016, 8, 1658-1664.	3.7	18
201	Alcohol-Induced Low-Temperature Blockage of Supported-Metal Catalysts for Enhanced Catalysis. ACS Catalysis, 2020, 10, 8515-8523.	11.2	18
202	Atomistic insights into the nucleation and growth of platinum on palladium nanocrystals. Nature Communications, 2021, 12, 3215.	12.8	18
203	An Application of Conformal Mapping to a Three-Dimensional Unsteady Heat Conduction Problem. Aeronautical Quarterly, 1965, 16, 221-230.	0.2	17
204	Threeâ€Dimensional Structural Analysis of MgO‣upported Osmium Clusters by Electron Microscopy with Singleâ€Atom Sensitivity. Angewandte Chemie - International Edition, 2013, 52, 5262-5265.	13.8	17
205	The effect of surface capping on the diffusion of adatoms in the synthesis of Pd@Au core–shell nanocrystals. Chemical Communications, 2016, 52, 13159-13162.	4.1	17
206	Novel Acid Catalysts from Wasteâ€Tireâ€Derived Carbon: Application in Waste–toâ€Biofuel Conversion. ChemistrySelect, 2017, 2, 4975-4982.	1.5	17
207	Segregation of Mn2+Dopants as Interstitials in SrTiO3Grain Boundaries. Materials Research Letters, 2014, 2, 16-22.	8.7	16
208	Rapid aberration measurement with pixelated detectors. Journal of Microscopy, 2016, 263, 43-50.	1.8	16
209	Facile Synthesis of Pt–Pd Alloy Nanocages and Pt Nanorings by Templating with Pd Nanoplates. ChemNanoMat, 2016, 2, 1086-1091.	2.8	16
210	Conversion of Waste Tire Rubber into High-Value-Added Carbon Supports for Electrocatalysis. Journal of the Electrochemical Society, 2018, 165, H881-H888.	2.9	16
211	Manipulating Copper Dispersion on Ceria for Enhanced Catalysis: A Nanocrystalâ€Based Atomâ€Trapping Strategy. Advanced Science, 2022, 9, e2104749.	11.2	16
212	Atomic and electronic structures of the SrVO3-LaAlO3 interface. Journal of Applied Physics, 2011, 110, 046104.	2.5	15
213	Understanding Strainâ€Induced Phase Transformations in BiFeO 3 Thin Films. Advanced Science, 2015, 2, 1500041.	11.2	15
214	NixWO2.72 nanorods as an efficient electrocatalyst for oxygen evolution reaction. Green Energy and Environment, 2017, 2, 119-123.	8.7	15
215	Rhodium Decahedral Nanocrystals: Facile Synthesis, Mechanistic Insights, and Experimental Controls. ChemNanoMat, 2018, 4, 66-70.	2.8	15
216	On the approximate solution of flow and heat transfer through non-circular conduits with uniform wall temperature. British Journal of Applied Physics, 1967, 18, 1327-1335.	0.7	14

#	Article	IF	CITATIONS
217	Comparison of Segregation Behaviors for Special and General Boundaries in Polycrystalline Al2O3with SiO2-TiO2Impurities. Journal of Materials Science, 2004, 12, 335-342.	1.2	14
218	Point defect characterization in HAADF-STEM images using multivariate statistical analysis. Ultramicroscopy, 2011, 111, 251-257.	1.9	14
219	A hollow Co2SiO4 nanosheet Li-ion battery anode with high electrochemical performance and its dynamic lithiation/delithiation using in situ transmission electron microscopy technology. Applied Surface Science, 2019, 490, 510-515.	6.1	14
220	Mechanistic understanding and strategies to design interfaces of solid electrolytes: insights gained from transmission electron microscopy. Journal of Materials Science, 2019, 54, 10571-10594.	3.7	14
221	Essential effect of the electrolyte on the mechanical and chemical degradation of LiNi _{0.8} Co _{0.15} Al _{0.05} O ₂ cathodes upon long-term cycling. Journal of Materials Chemistry A, 2021, 9, 2111-2119.	10.3	14
222	Sidewall Morphology-Dependent Formation of Multiple Twins in Si Nanowires. ACS Nano, 2013, 7, 8206-8213.	14.6	13
223	Quantifying stoichiometry-induced variations in structure and energy of a SrTiO ₃ symmetric Σ13 {510}/<100 > grain boundary. Philosophical Magazine, 2013, 1219-1229.	931.6	13
224	Improving superconductivity in BaFe2As2-based crystals by cobalt clustering and electronic uniformity. Scientific Reports, 2017, 7, 949.	3.3	13
225	Pd@Rh core–shell nanocrystals with well-defined facets and their enhanced catalytic performance towards CO oxidation. Nanoscale Horizons, 2019, 4, 1232-1238.	8.0	13
226	Pt–Co truncated octahedral nanocrystals: a class of highly active and durable catalysts toward oxygen reduction. Nanoscale, 2020, 12, 11718-11727.	5.6	13
227	Machine Learning Method Reveals Hidden Strong Metalâ€Support Interaction in Microscopy Datasets. Small Methods, 2021, 5, 2100035.	8.6	13
228	Neutron diffraction study of magnetism in van der Waals layered MnBi _{2n } Te _{3n+1} . Journal Physics D: Applied Physics, 2021, 54, 174003.	2.8	13
229	Interferometric 4Dâ€STEM for Lattice Distortion and Interlayer Spacing Measurements of Bilayer and Trilayer 2D Materials. Small, 2021, 17, e2100388.	10.0	13
230	Iridiumâ€Based Cubic Nanocages with 1.1â€nmâ€Thick Walls: A Highly Efficient and Durable Electrocatalyst for Water Oxidation in an Acidic Medium. Angewandte Chemie, 2019, 131, 7322-7326.	2.0	12
231	Enhanced alcohol production over binary Mo/Co carbide catalysts in syngas conversion. Journal of Catalysis, 2020, 391, 446-458.	6.2	12
232	Triosmium Clusters on a Support: Determination of Structure by Xâ€ray Absorption Spectroscopy and Highâ€Resolution Microscopy. Chemistry - A European Journal, 2011, 17, 1000-1008.	3.3	11
233	Grain boundary stability and influence on ionic conductivity in a disordered perovskite—a first-principles investigation of lithium lanthanum titanate. MRS Communications, 2016, 6, 455-463.	1.8	11
234	Facile Synthesis of Pt Icosahedral Nanocrystals with Controllable Sizes for the Evaluation of Sizeâ€Dependent Activity toward Oxygen Reduction. ChemCatChem, 2019, 11, 2458-2463.	3.7	11

#	Article	IF	CITATIONS
235	Maximizing the Catalytic Performance of Pd@Au _x Pd _{1â^'<i>x</i>} Nanocubes in H ₂ O ₂ Production by Reducing Shell Thickness to Increase Compositional Stability. Angewandte Chemie, 2021, 133, 19795-19799.	2.0	11
236	Transverse and torsional vibrations of an axially-loaded beam with elastically constrained ends. Journal of Sound and Vibration, 1984, 96, 235-241.	3.9	10
237	Novel Solid Electrolytes for Li-Ion Batteries: A Perspective from Electron Microscopy Studies. Frontiers in Energy Research, 2016, 4, .	2.3	10
238	Optimizing the structural configuration of FePt-FeOx nanoparticles at the atomic scale by tuning the post-synthetic conditions. Nano Energy, 2019, 55, 441-446.	16.0	10
239	Engineering Tunneling Selector to Achieve High Non-linearity for 1S1R Integration. Frontiers in Nanotechnology, 2021, 3, .	4.8	10
240	Robust Atomic-Resolution Imaging of Lithium in Battery Materials by Center-of-Mass Scanning Transmission Electron Microscopy. ACS Nano, 2022, 16, 1358-1367.	14.6	10
241	Dimensionality Effects in FeGe2 Nanowires: Enhanced Anisotropic Magnetization and Anomalous Electrical Transport. Scientific Reports, 2017, 7, 7126.	3.3	9
242	An all-in-one Sn–Co alloy as a binder-free anode for high-capacity batteries and its dynamic lithiation in situ. Chemical Communications, 2019, 55, 529-532.	4.1	9
243	Effect of TiO2–SiO2distribution on bimodal microstructure of TiO2-doped α-Al2O3ceramics. International Journal of Materials Research, 2005, 96, 486-492.	0.8	8
244	Facile Synthesis of Ag@Pd _{nL} Icosahedral Nanocrystals as a Class of Costâ€Effective Electrocatalysts toward Formic Acid Oxidation. ChemCatChem, 2020, 12, 5156-5163.	3.7	8
245	Highâ€Performance Lithium Solidâ€State Batteries Operating at Elevated Temperature. Advanced Materials Interfaces, 2015, 2, 1500268.	3.7	7
246	A novel tin hybrid nano-composite with double nets of carbon matrixes as a stable anode in lithium ion batteries. Chemical Communications, 2017, 53, 13125-13128.	4.1	7
247	Real Space Visualization of Competing Phases in La0.6Sr2.4Mn2O7 Single Crystals. Chemistry of Materials, 2018, 30, 7962-7969.	6.7	7
248	Migration of Cobalt Species within Mixed Platinum-Cobalt Oxide Bifunctional Electrocatalysts in Alkaline Electrolytes. Journal of the Electrochemical Society, 2019, 166, F3093-F3097.	2.9	7
249	Swellingâ€Induced Symmetry Breaking: A Versatile Approach to the Scalable Production of Colloidal Particles with a Janus Structure. Angewandte Chemie, 2021, 133, 13090-13094.	2.0	7
250	Phase-Controlled Synthesis of Ru Nanocrystals via Template-Directed Growth: Surface Energy versus Bulk Energy. Nano Letters, 2022, 22, 3591-3597.	9.1	7
251	Atomically Dispersed Platinum in Surface and Subsurface Sites on MgO Have Contrasting Catalytic Properties for CO Oxidation. Journal of Physical Chemistry Letters, 2022, 13, 3896-3903.	4.6	7
252	Tantalum Clusters Supported on Silicaâ^'Alumina: Influence of Support Composition and Chemistry on Cluster Structure. Langmuir, 2009, 25, 10754-10763.	3.5	6

#	Article	IF	CITATIONS
253	The Application of Scanning Transmission Electron Microscopy (STEM) to the Study of Nanoscale Systems. Nanostructure Science and Technology, 2012, , 11-40.	0.1	6
254	Redox-couple investigations in Si-doped Li-rich cathode materials. Physical Chemistry Chemical Physics, 2021, 23, 2780-2791.	2.8	6
255	Ultrasound-mediated synthesis of nanoporous fluorite-structured high-entropy oxides toward noble metal stabilization. IScience, 2022, 25, 104214.	4.1	6
256	A sketch-based collaborative design system. , 0, , .		5
257	Frank dislocation loops in HgTeâ^•CdTe superlattices on CdTeâ^•Si(211)B substrates. Journal of Applied Physics, 2008, 104, 023104.	2.5	5
258	Computer-Controlled In Situ Gas Reactions via a MEMS-based Closed-Cell System. Microscopy and Microanalysis, 2015, 21, 97-98.	0.4	5
259	Revealing the Preferred Interlayer Orientations and Stackings of Twoâ€Dimensional Bilayer Gallium Selenide Crystals. Angewandte Chemie, 2015, 127, 2750-2755.	2.0	5
260	Conduction below 100°C in nominal Li6ZnNb4O14. Journal of Materials Science, 2016, 51, 854-860.	3.7	5
261	A Simple Route to the Synthesis of Pt Nanobars and the Mechanistic Understanding of Symmetry Reduction. Chemistry - A European Journal, 2021, 27, 2760-2766.	3.3	5
262	Plasma charging damage on silicon surface during reverse-AA oxide etching in poly-buffered STI (PB-STI) isolation process. , 0, , .		4
263	Microstructural evolution of protective La–Cr–O films studied by transmission electron microscopy. Journal of Solid State Electrochemistry, 2006, 10, 659-662.	2.5	4
264	Ptychographic Imaging in an Aberration Corrected STEM. Microscopy and Microanalysis, 2015, 21, 1219-1220.	0.4	4
265	Metallicity of Ca2Cu6P5 with single and double copper-pnictide layers. Journal of Alloys and Compounds, 2016, 671, 334-339.	5.5	4
266	Machine Learning for Challenging EELS and EDS Spectral Decomposition. Microscopy and Microanalysis, 2019, 25, 180-181.	0.4	4
267	Emerging Electron Microscopy Techniques for Probing Functional Interfaces in Energy Materials. Angewandte Chemie, 2020, 132, 1400-1412.	2.0	4
268	Response of slender structural members in self-excited oscillation. Journal of Sound and Vibration, 1985, 101, 75-83.	3.9	3
269	Interface structure and transport of complex oxide junctions. Journal of Vacuum Science & Technology B, 2008, 26, 1521.	1.3	3
270	Understanding Surface Modification and Electrochemical Cycling Stability of Oxide Cathode Materials for Li-Ion Batteries by Advanced Analytical Transmission Electron Microscopy. Microscopy and Microanalysis, 2011, 17, 1574-1575.	0.4	3

#	Article	IF	CITATIONS
271	Functional Electron Microscopy for Electrochemistry Research: From the Atomic to the Micro Scale. Electrochemical Society Interface, 2014, 23, 61-66.	0.4	3
272	Facile Synthesis of BaTiO ₃ Nanocubes with the Use of Anatase TiO ₂ Nanorods as a Precursor to Titanium Hydroxide. ChemNanoMat, 2016, 2, 873-878.	2.8	3
273	Facile synthesis of Pt–Ag octahedral and tetrahedral nanocrystals with enhanced activity and durability toward methanol oxidation. Journal of Materials Research, 2018, 33, 3891-3897.	2.6	3
274	<i>In situ</i> Electric Field Manipulation of Ferroelectric Vortices. Microscopy and Microanalysis, 2019, 25, 1844-1845.	0.4	3
275	Probing the Origin of Microcracks in Layered Oxide Cathodes via Electron Microscopy. Microscopy and Microanalysis, 2019, 25, 2058-2059.	0.4	3
276	Infrared optical absorption of iridium silicide films on silicon. Journal of Applied Physics, 1994, 76, 3028-3031.	2.5	2
277	Contact size dependence of highly selective self-aligned contact etching with polymer formation and its mechanism. , 0, , .		2
278	The Emergence of Intergranular Precipitates in TiO2-Doped α-Al2O3Ceramics. Journal of the American Ceramic Society, 2010, 93, 326-329.	3.8	2
279	Templated one-step catalytic fabrication of uniform diameter MgxBy nanostructures. Journal of Materials Chemistry C, 2013, 1, 2568.	5.5	2
280	Recent Development of Platinum-Based Nanocatalysts for Oxygen Reduction Electrocatalysis. Nanostructure Science and Technology, 2016, , 253-280.	0.1	2
281	Using Multivariate Analysis of Scanning-Rochigram Data to Reveal Material Functionality. Microscopy and Microanalysis, 2016, 22, 292-293.	0.4	2
282	Accurate Calculation of CBED Patterns for 4D STEM Using Electron Densities Calculated by Density Functional Theory Microscopy and Microanalysis, 2018, 24, 116-117.	0.4	2
283	Atomic-Scale Structural Mapping of Active Sites in Monolayer PGM-Free Catalysts by Low-Voltage 4D-STEM. Microscopy and Microanalysis, 2020, 26, 162-163.	0.4	2
284	Machine Learning: Machine Learning Method Reveals Hidden Strong Metal‧upport Interaction in Microscopy Datasets (Small Methods 5/2021). Small Methods, 2021, 5, 2170020.	8.6	2
285	Correlating inhomogeneity in anionic electron density with hydrogen incorporation in Y5Si3 electrides. Microscopy and Microanalysis, 2021, 27, 146-147.	0.4	2
286	Li0.625Al0.125H0.25Cl0.75O0.25 Superionic Conductor with Disordered Rock-Salt Structure. ACS Applied Energy Materials, 2021, 4, 7674-7680.	5.1	2
287	Non-linear forced vibration of a non-prismatic beam due to combined flexure and stretching. Journal of Sound and Vibration, 1971, 15, 447-454.	3.9	1
288	Quenching of photoconductivity in silver sulfide thin layers by ultraviolet radiation. Applied Physics Letters, 1978, 32, 543-545.	3.3	1

#	Article	lF	CITATIONS
289	Misfit Dislocations in Ferroelectric Thin films. Microscopy and Microanalysis, 2008, 14, 240-241.	0.4	1
290	Atomic Scale EELS Study of the Origin of Ferromagnetism in Co doped ZnO Epitaxial Thin Films. Microscopy and Microanalysis, 2009, 15, 436-437.	0.4	1
291	Investigation of Nanostructure and Photocatalytic Stability of Mesoporous CuCrO2 Delafossite using Analytical Electron Microscopy. Microscopy and Microanalysis, 2009, 15, 1406-1407.	0.4	1
292	Novel Closed-Cell Gas-Reaction Holder Allows Characterization of Behavior of Bimetallic Nanoparticles at Elevated Temperatures and Gas Pressures. Microscopy and Microanalysis, 2013, 19, 1474-1475.	0.4	1
293	Fast Aberration Measurement in Multi-Dimensional STEM. Microscopy and Microanalysis, 2016, 22, 252-253.	0.4	1
294	Atomic-resolution electric field measurements with a universal detector. Microscopy and Microanalysis, 2018, 24, 114-115.	0.4	1
295	Nanoscale interlayer defects in iron arsenides. Journal of Solid State Chemistry, 2019, 277, 422-426.	2.9	1
296	Electromagnetic Field Reconstructions of 4D-STEM Datasets using Ptychography and Differential Phase Contrast Imaging. Microscopy and Microanalysis, 2019, 25, 66-67.	0.4	1
297	Cryogenic Atomic Resolution and 4D STEM Imaging for Energy and Quantum Materials. Microscopy and Microanalysis, 2021, 27, 384-385.	0.4	1
298	Microscopy Society of America Awards: 2021 Award Winners. Microscopy Today, 2021, 29, 10-15.	0.3	1
299	Synthesis and Characterization of Ptâ€Ag Icosahedral Nanocages with Enhanced Catalytic Activity toward Oxygen Reduction. ChemNanoMat, 0, , .	2.8	1
300	Reply to â€~Comments on "Response of oddly-stiffened circular cylindrical shellsâ€â€™. Journal of Sound and Vibration, 1972, 21, 246-247.	3.9	0
301	Applications of Atomic Scale Scanning Transmission Electron Microscopy. Microscopy and Microanalysis, 2006, 12, 134-135.	0.4	0
302	Studying Vanadium-based Perovskites by Scanning Transmission Electron Microscopy. Microscopy and Microanalysis, 2006, 12, 1178-1179.	0.4	0
303	A TEM Study on the Doping Behavior of Calcium in LaCoO3. Microscopy and Microanalysis, 2006, 12, 728-729.	0.4	0
304	Structure and Size Determination of the Metal Nanoclusters in the Supported Catalyst: Os3/MgO by Z-Contrast Imaging. Microscopy and Microanalysis, 2010, 16, 1186-1187.	0.4	0
305	An Investigation of Structure and Electrochemical Cycle Stability of Li[Li0.2Ni0.2Mn0.6]O2 by using Aberration Corrected Z-contrast Imaging and EELS. Microscopy and Microanalysis, 2010, 16, 78-79.	0.4	0
306	Practical Aspects of Atomic-Scale In Situ Investigation of Electrochemistry in All-Solid Lithium-Ion Batteries. Microscopy and Microanalysis, 2012, 18, 1404-1405.	0.4	0

#	Article	IF	CITATIONS
307	Phase Transitions, Phase Coexistence, and Piezoelectric Switching Behavior in Highly Strained BiFeO3Films (Adv. Mater. 39/2013). Advanced Materials, 2013, 25, 5560-5560.	21.0	0
308	Examining Atomistic Defect-Boundary Interactions Induced by Ion Irradiation using Aberration Corrected Transmission Electron Microscopy. Microscopy and Microanalysis, 2013, 19, 1982-1983.	0.4	0
309	In-situ Atomic-scale Investigation of Elemental Diffusion in Pt-Co Nanoparticles. Microscopy and Microanalysis, 2013, 19, 1460-1461.	0.4	0
310	STEM in 4 Dimensions: Using Multivariate Analysis of Ptychographic Data to Reveal Material Functionality. Microscopy and Microanalysis, 2015, 21, 1863-1864.	0.4	0
311	Atomic Resolution STEM-EELS Study of Transition Electronic Localization State Induced by Strain. Microscopy and Microanalysis, 2015, 21, 617-618.	0.4	0
312	Microscopy Guided Design of Radial p-n Junction in Single TiO2 Nanotubes. Microscopy and Microanalysis, 2015, 21, 1741-1742.	0.4	0
313	Evolution of Au 25 (SR)18 Nanoclusters on Ceria Surfaces during in situ Electron Beam Irradiation. Microscopy and Microanalysis, 2016, 22, 1278-1279.	0.4	0
314	Scalable Synthesis of Palladium Icosahedra in Plug Reactors for the Production of Oxygen Reduction Reaction Catalysts. ChemCatChem, 2016, 8, 1602-1602.	3.7	0
315	A "Hidden―Mesoscopic Feature Revealed By Electron Microscopy Could Facilitate Ion Transport In Solid Electrolytes. Microscopy and Microanalysis, 2016, 22, 1308-1309.	0.4	0
316	Integrating Novel Microscopy into Battery Research: From Atomic Resolution to In Situ and Functional Imaging. Microscopy and Microanalysis, 2017, 23, 1998-1999.	0.4	0
317	Elucidating Ion Transport in Lithium-Ion Conductors by Combining Vibrational Spectroscopy in STEM and Neutron Scattering. Microscopy and Microanalysis, 2018, 24, 1496-1497.	0.4	0
318	Atomic-Scale Study of Intrinsic Defects Suppressing the Thermal Conductivity of Boron Arsenide. Microscopy and Microanalysis, 2019, 25, 942-943.	0.4	0
319	Mapping Local Structural and Electronic Properties of 2D Materials by Multi-dimensional STEM. Microscopy and Microanalysis, 2019, 25, 960-961.	0.4	0
320	Stabilizing Fuel Cell Materials Through Cryogenic Cooling for Simultaneous EELS-EDS Analysis. Microscopy and Microanalysis, 2020, 26, 1660-1662.	0.4	0
321	Elastic deformations in strips with holes loaded through pins. Journal of Research of the National Bureau of Standards, 1959, 62, 147.	0.4	0